

Citation for published version:

Gorbach, AV, Marini, A & Skryabin, DV 2013, 'Graphene-clad tapered fiber: Effective nonlinearity and propagation losses', *Optics Letters*, vol. 38, no. 24, pp. 5244-5247. <https://doi.org/10.1364/OL.38.005244>

DOI:

[10.1364/OL.38.005244](https://doi.org/10.1364/OL.38.005244)

Publication date:

2013

Document Version

Peer reviewed version

[Link to publication](#)

This paper was published in Optics Letters and is made available as an electronic reprint with the permission of OSA. The paper can be found at the following URL on the OSA website: <http://dx.doi.org/10.1364/OL.38.005244>. Systematic or multiple reproduction or distribution to multiple locations via electronic or other means is prohibited and is subject to penalties under law.

University of Bath

Alternative formats

If you require this document in an alternative format, please contact:
openaccess@bath.ac.uk

General rights

Copyright and moral rights for the publications made accessible in the public portal are retained by the authors and/or other copyright owners and it is a condition of accessing publications that users recognise and abide by the legal requirements associated with these rights.

Take down policy

If you believe that this document breaches copyright please contact us providing details, and we will remove access to the work immediately and investigate your claim.

Graphene-clad tapered fibre: effective nonlinearity and propagation losses

A. V. Gorbach,^{1,*} A. Marini,² and D. V. Skryabin¹

¹Centre for Photonics and Photonic Materials, Department of Physics, University of Bath, Bath BA2 7AY, UK

²Max Planck Institute for the Science of Light, Guenther-Scharowsky-Straße 1, 91058 Erlangen, Germany

compiled: December 2, 2013

We derive pulse propagation equation for a graphene-clad optical fibre, treating optical response of graphene and nonlinearity of the dielectric fibre core as perturbations in asymptotic expansion of Maxwell equations. We analyse the effective nonlinear and attenuation coefficients due to the graphene layer. Based on the recent experimental measurements of the nonlinear graphene conductivity, we predict considerable enhancement of the effective nonlinearity for sub-wavelength fibre core diameters.

OCIS codes: (190.4370) Nonlinear optics, fibers; (190.3270) Kerr effect; (160.4330) Nonlinear optical materials; (160.4236) Nanomaterials.

<http://dx.doi.org/10.1364/XX.99.099999>

Optical and opto-electronic properties of graphene attract much attention in recent years [1, 2]. In particular, the effective optical nonlinearity of graphene is predicted to be very high [3, 4]. This is supported by recent experiments, including direct measurements of the effective χ_3 of graphene with optical Kerr gate [5] and z-scan [6] techniques, as well as observation of four-wave mixing [7] and higher harmonics generation [8–10] in mono- and few-layer graphene samples. The values of the nonlinear susceptibility of graphene derived from experimental data are reported to be as high as $10^{-16} m^2/V^2$ [7, 8] in infrared spectral range, i.e. exceeding values for typical dielectrics by 5-6 orders of magnitude. This finding makes graphene a promising material for nonlinear optics and photonic. Recently, generation of spatial solitons was predicted in graphene-core planar dielectric waveguide [11] and graphene-semiconductor layered structures [12], as well as nonlinear self-focusing [13] and switching [14] of graphene plasmons at sub-wavelength scale. Significant enhancement of a range of nonlinear processes, including four-wave mixing, was observed experimentally in a graphene-clad semiconductor photonic crystal cavity [15].

In this Letter we consider a graphene-clad tapered fibre, see Fig. 1. If the core radius of the fibre R is tapered down to the wavelength scale, the then a large proportion of light being guided at the outer boundary and outside the fibre [16], see Fig. 1(b). This ensures good field overlap with the graphene layer, so as to maximize its contribution to the overall effective nonlinearity of the

structure. The primary aim of this work is to characterize the corresponding nonlinearity enhancement and estimate propagation losses due to the graphene-induced photon absorptions.

To analyse pulse propagation in the structure, it is convenient to use Fourier expansion of the total electric field:

$$\vec{\mathcal{E}}(\vec{r}, t) = \frac{1}{\sqrt{2\pi}} \int_{-\infty}^{+\infty} \mathbf{E}(\vec{r}, \omega) e^{-i\omega t} d\omega + c.c. \quad (1)$$

We assume that the mode profile is practically not affected by the addition of the atom-thick graphene layer to the fibre boundary, and describe each complex harmonic by means of a slowly varying envelope $A_\omega(z)$ of the corresponding linear guided mode \mathbf{e}_ω of the bare fibre:

$$E(r, \phi, z, \omega) = A_\omega(z) \mathbf{e}_\omega(r, \phi), \quad (2)$$

Hereafter cylindrical system of coordinates (r, ϕ, z) is used. Adopting complex harmonic amplitudes for the displacement vector \mathcal{D} and induced current \mathcal{J} similarly to the electric field, Eq. (1), nonlinear optical response of the dielectric core and graphene layer can be written as [13, 17]:

$$\mathbf{D}(\omega) = \epsilon_0 \epsilon \mathbf{E}(\omega) + \epsilon_0 \hat{\chi}^{(3)} : \mathbf{E}(\omega_1) \mathbf{E}^*(\omega_2) \mathbf{E}(\omega_3), \quad (3)$$

$$\mathbf{J}(\omega) = \hat{\sigma}^{(1)} \mathbf{J}(\omega) + \hat{\sigma}^{(3)} : \mathbf{J}(\omega_1) \mathbf{J}^*(\omega_2) \mathbf{J}(\omega_3), \quad (4)$$

where $\omega_3 = \omega - \omega_1 + \omega_2$, nonlinear susceptibility tensor is given by: $\hat{\chi}_{ipjs}^{(3)} = (\chi_3/3) [\delta_{ip}\delta_{js} + \delta_{ij}\delta_{ps} + \delta_{is}\delta_{pj}]$, δ_{ij} is the Kronecker's delta. Considering graphene as a 2D material, we assume a similar structure of the nonlinear

* Corresponding author: A.Gorbach@bath.ac.uk

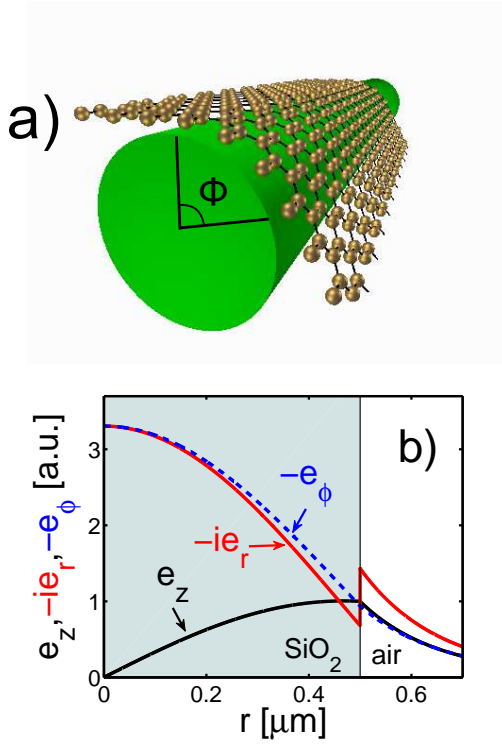


Fig. 1. (Color online) A tapered fibre partially covered with graphene: (a) schematic view, the overlap spans the angle Φ , $0 < \Phi < 2\pi$; (b) fundamental mode profile of the bare silica glass fibre with core diameter $2R = \lambda_0 = 1\mu\text{m}$.

conductivity tensor, but with the indexes i, p, j, s each corresponding to ϕ or z only. Also, the symmetry of graphene and the requirement $J_r = 0$, still permit six additional non-zero tensor components $\hat{\sigma}_{jrrr}^{(3)} = \hat{\sigma}_{jrjr}^{(3)} = \hat{\sigma}_{jrrj}^{(3)} = \tilde{\sigma}_3/3$, $j = z, \phi$. In absence of external magnetic fields, linear conductivity tensor has only two non-zero components: $\hat{\sigma}_{\phi\phi}^{(1)} = \hat{\sigma}_{zz}^{(1)} = \sigma_1$.

Performing asymptotic expansion of Maxwell equations, where optical response of the graphene layer and nonlinearity due to the dielectric fibre core are treated as perturbations, and following similar steps as described in details in our recent works [13, 18], for the envelopes A_ω we eventually derive the following equation:

$$i\partial_z A_\omega = -(d_\omega + i\alpha_\omega)A_\omega - \frac{\omega}{2\pi} \int_{-\infty}^{\infty} \int_{-\infty}^{\infty} \Gamma A_{\omega_1} A_{\omega_2}^* A_{\omega_3} d\omega_1 d\omega_2, \quad (5)$$

$$d_\omega = \beta(\omega) + \nu(\omega), \quad (6)$$

Here β is the propagation constant of the bare fibre mode [18], while ν and α represent corrections to its real and imaginary (attenuation) parts due to the graphene layer. Nonlinear coefficient Γ generally depends on the four frequencies $\omega, \omega_1, \omega_2, \omega_3$ and contains information about the material and geometrical dispersion of the nonlinearity [17]. This dependence only becomes important for ultra-short pulses [19] or wide bandwidth frequency con-

version processes [17]. Considering narrow-bandwidth pulses, we replace Γ with a constant value Γ_0 computed at the pulse central frequency ω_0 . Then, performing inverse Fourier transform of Eq. (6), introducing slowly varying pulse envelope $A(z, t)$:

$$A(z, t) = \frac{1}{\sqrt{2\pi}} \int_{-\infty}^{+\infty} A_\omega(z) e^{-i(\omega_0 + \delta)t} d\delta, \quad (7)$$

and shifting to the moving frame $A(z, t) = I^{-1/2} \psi(z, \tau = t - v_g^{-1}z) e^{i\delta_0 z}$, the following pulse propagation equation is obtained:

$$i\partial_z \psi + \hat{D}(i\partial_\tau) \psi + i\hat{\Lambda}(i\partial_\tau) \psi + \gamma |\psi|^2 \psi = 0, \quad (8)$$

where dispersion \hat{D} and attenuation $\hat{\Lambda}$ operators are defined through coefficients d_k and α_k of the polynomial fits of the propagation constant $d(\delta) = \sum_{k=0}^N \frac{d_k}{k!} \delta^k$ and attenuation coefficient $\alpha(\delta) = \sum_{k=0}^N \frac{\alpha_k}{k!} \delta^k$, respectively:

$$\hat{D} = \sum_{k=2}^N \frac{d_k}{k!} (i\partial_\tau)^k, \quad \hat{\Lambda} = \sum_{k=0}^N \frac{\alpha_k}{k!} (i\partial_\tau)^k, \quad (9)$$

$v_g^{-1} = d_1$, $I^{-1/2}$ is the normalization factor to ensure that $|\psi|^2$ gives power (in watts) carried in the z direction [13, 17]. Graphene-induced corrections to the propagation constant ν and the attenuation coefficient α are given by:

$$(\nu + i\alpha) = f \sqrt{g} \frac{\pi k_0 R}{\beta_0 P} \frac{i\sigma_1}{c\epsilon_0} \Theta [|e_z|^2 + |e_\phi|^2], \quad (10)$$

and the nonlinear coefficient γ combines contributions from the dielectric core [18] and graphene:

$$\gamma = \gamma_D + \gamma_G, \quad (11)$$

$$\gamma_D = g \frac{\pi k_0^3}{\beta_0^2 P^2} \frac{\chi_3}{c\epsilon_0} \int_0^R r \left[|\vec{e}|^4 + \frac{1}{2} |\vec{e}^2|^2 \right] dr, \quad (12)$$

$$\gamma_G = f g \frac{\pi k_0^3}{\beta_0^2 P^2} \frac{i\sigma_3}{(c\epsilon_0)^2} \frac{R}{k_0} \Theta \left[|\vec{e}_1|^4 |\vec{e}_{||}|^2 + \frac{1}{2} \vec{e}_1^2 (\vec{e}_{||}^*)^2 \right] \quad (13)$$

Here $k_0 = \omega_0/c$, R is the fibre radius, factor $f = \Phi/(2\pi)$ characterizes overlap between the fibre and the graphene layer, see Fig. 1(a), $\vec{e}_{||} = [e_z, e_\phi]^T$, $\vec{e}_1 = [\tilde{s}e_r, e_z, e_\phi]^T$, $\tilde{s} = (\tilde{\sigma}_3/\sigma_3)^{0.5}$, normalization factor P is:

$$P = 2\pi \int_0^{+\infty} r |\vec{e}|^2 dr, \quad (14)$$

g is the surface enhancement factor [18]:

$$g = 1/(1 + \eta)^2, \quad (15)$$

$$\eta = \frac{2\pi R}{\beta_0 P} \Delta [e_r^* e_z], \quad (16)$$

and operators Θ and Δ are defined as:

$$\Theta[F(r)] = \frac{1}{2} \lim_{\delta r \rightarrow 0} [F(R - \delta r) + F(R + \delta r)], \quad (17)$$

$$\Delta[F(r)] = \lim_{\delta r \rightarrow 0} [F(R - \delta r) - F(R + \delta r)]. \quad (18)$$

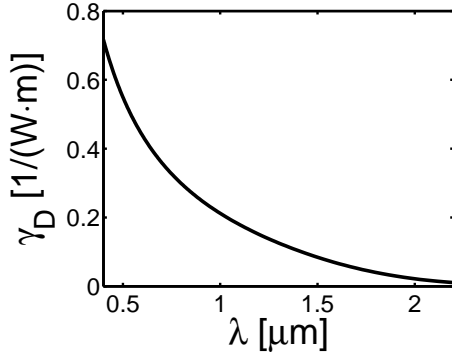


Fig. 2. Nonlinear coefficient of the fundamental mode of the silica glass fibre with $R = 0.5\mu\text{m}$, $\chi_3 = 4 \cdot 10^{-22} \text{m}^2/\text{V}^2$.

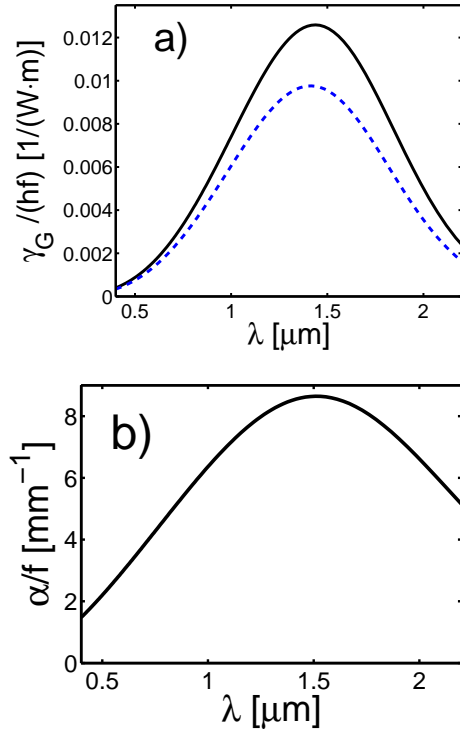


Fig. 3. (Color online) Graphene contribution to the nonlinearity (a) and propagation loss (b). Solid (dashed) curve in (a) corresponds to $\tilde{s} = 1$ ($\tilde{s} = 0$).

Below we consider a silica glass fibre with the diameter $2R = 1\mu\text{m}$ [16]. The corresponding nonlinear coefficient γ_D is plotted in Fig. 2. When the core radius R is smaller than the wavelength, nonlinearity of the dielectric fibre monotonically decreases with λ .

For a typical graphene sample with a chemical potential of the order of $\mu = 0.1\text{eV}$ [15], the considered range of wavelengths falls beyond the absorption threshold in graphene ($\lambda_{th} = 2\pi c/\omega_{th} = \pi c\hbar/\mu \approx 6\mu\text{m}$). In this regime, a considerable impact of the graphene layer on the mode dispersion is expected to be through the

increased attenuation, associated with the real part of linear conductivity $\text{Re}(\sigma_1) = e^2/(4\hbar)$ [20]. We are not aware of a theoretical derivation or experimental measurement of the nonlinear graphene conductivity coefficients σ_3 and $\tilde{\sigma}_3$ at frequencies above the chemical potential. For convenience, we introduce the dimensionless coefficient:

$$h = \frac{\chi_3^{(gr)}}{\chi_3} = \frac{\sigma_3}{c\epsilon_0\chi_3}, \quad (19)$$

which characterizes the relative strength of Kerr effect in graphene.

The graphene contributions to the nonlinear and loss coefficients are plotted in Fig. 3. The impact of graphene on nonlinearity and attenuation achieves its maximum at a wavelength around $1.5\mu\text{m}$, i.e. when the fibre diameter is about 1.5 times smaller than the wavelength in vacuum. While geometrical dispersion largely dominates over material dispersion in such small-core fibres, similar results are obtained for a fixed wavelength and varying fibre diameter. The account of possible dependance of graphene conductivity on the orthogonal component of applied field ($\tilde{\sigma}_3 \neq 0$) changes γ_G only slightly, cf. solid and dashed curves in Fig. 3(a).

To estimate the enhancement of nonlinearity due to the graphene layer, we rely on the indirect experimental measurements of σ_3 in infrared wavelength range [7, 8, 15]. In all the above experiments effective nonlinear susceptibility of graphene $\chi_3^{(gr)}$ is defined in the same way as for a bulk material, assuming certain thickness of the graphene layer, and therefore it is different from our definition in Eq. (19). From experimental data reported by Hendry et al. [7] and Kumar et al. [8] we estimate $\sigma_3 \sim 10^{-22} \text{Sm}/\text{V}^2$, and therefore $h \sim 10^4$. With such a strong relative nonlinear susceptibility of graphene, γ_G and γ_D at wavelengths around $\lambda_0 = 2\pi/k_0 = 1\mu\text{m}$ become comparable for the overlap factor $f \sim 0.01$. And the effective graphene nonlinearity of a fully wrapped fibre ($f = 1$) can exceed the nonlinearity due to the dielectric core by more than two orders of magnitude, cf. Figs. 2 and 3(a). This prediction is consistent with the measured boost of Kerr nonlinearity in a graphene-clad silicon photonic crystal cavity [15].

Graphene induced propagation losses introduce major limitations to the overall nonlinear performance of the fibre. For wavelengths around $1\mu\text{m}$ and angular overlap rate of $f = 0.1$, typical attenuation distances $L_a = 1/\alpha$ are found to be of the order of few mm, cf. Fig. 3(b). This needs to be compared with the characteristic nonlinear distance $L_{NL} = 1/(\gamma_G P)$ required to observe the graphene-induced additional nonlinear phase shift of a pulse. In Fig. 4 we plot the peak power P required to match the two distances. It is easy to see that this power does not depend on the overlap factor f and is defined only by the relative strength of the graphene nonlinearity h . For the estimated above value of $h \sim 10^4$, one should be able to observe the additional phase shift at peak powers as low as few hundred watts. However for

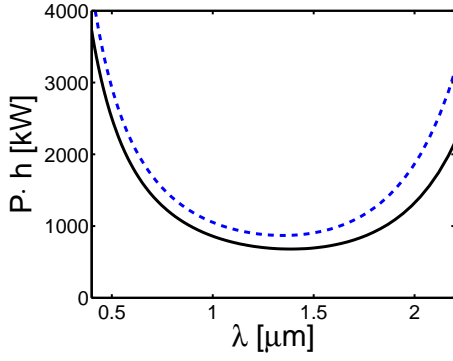


Fig. 4. (Color online) Power required to match nonlinear and attenuation distances. Solid (dashed) curve corresponds to $\tilde{s} = 1$ ($\tilde{s} = 0$).

smaller h , as the peak power raises up to few kW, electric field at the edge of the fibre may reach the graphene breakdown threshold $E_{cr} \sim 10^9 \text{ V/m}$ [21]. A much better balance between nonlinearity and attenuation could be achieved with highly-doped graphene samples, such as e.g. produced by chemical vapour deposition method [22]. As the chemical potential rises above 0.6 eV , the corresponding absorption threshold is shifted down to $\lambda_{th} \sim 1 \mu\text{m}$. This allows to reduce the attenuation substantially.

Note, that the propagation Eq. (8) could be derived by using an asymptotic expansion approach based on the reciprocity theorem [17, 23–25], provided one introduces the effective polarization of graphene using the same expression as in Eq. (3) and with the following effective linear and nonlinear susceptibility tensors:

$$\hat{\epsilon}_g = \frac{i\hat{\sigma}^{(1)}}{c\epsilon_0} \cdot \frac{c}{\omega} \delta(r - R_g), \quad (20)$$

$$\hat{\chi}_g^{(3)} = \frac{i\hat{\sigma}^{(3)}}{c\epsilon_0} \cdot \frac{c}{(\omega_1\omega_2\omega_3)^{1/3}} \delta(r - R_g). \quad (21)$$

Here $\delta(r)$ is the Dirac δ function, $R_g(\phi)$ is the position of graphene layer. It is easy to see that these expressions can be used in more complicated geometries without radial symmetry.

In summary, using the asymptotic expansion of Maxwell equations with nonlinear boundary condition, we derived propagation equation that describes nonlinear pulse dynamics in a graphene-clad dielectric fibre. Using experimental data for indirect measurements of the nonlinear graphene conductivity in infrared spectral range, we predict boosts of the effective nonlinearity by 2-3 orders of magnitude for fibre diameters below the carrier wavelength in vacuum. The associated nonlinear phase shifts could be observed for input powers below the graphene damage threshold and at short enough propagation distances to overcome limitations induced by high attenuation in graphene. We anticipate that a graphene layer could be fixed on the fibre wall by using similar wet-transport technique as in Ref. [15]. The

setup could be used to experimentally measure nonlinear conductivity of graphene as a function of frequency and chemical potential. Using the derived expressions for the effective linear and nonlinear susceptibilities of graphene, Eqs. (20), (21), it is straightforward to apply our method to other geometries such as graphene-clad semiconductor nano-wires.

References

- [1] F. Bonaccorso, Z. Sun, T. Hasan, and A. C. Ferrari, *Nature Photonics* **4**, 611 (2010).
- [2] Q. Bao and K. P. Loh, *ACS Nano* **6**, 3677 (2012).
- [3] S. A. Mikhailov, *Eur. Phys. Lett.* **79**, 27002 (2007).
- [4] S. A. Mikhailov and K. Ziegler, *Journal of physics. Condensed matter* **20**, 384204 (2008).
- [5] S. Chu, S. Wang, and Q. Gong, *Chem. Phys. Lett.* **523**, 104 (2011).
- [6] H. Zhang, S. Virally, Q. Bao, L. Kian Ping, S. Massar, N. Godbout, and P. Kockaert, *Opt. Lett.* **37**, 1856 (2012).
- [7] E. Hendry, P. J. Hale, J. Moger, A. K. Savchenko, and S. A. Mikhailov, *Phys. Rev. Lett.* **105**, 097401 (2010).
- [8] N. Kumar, J. Kumar, C. Gerstenkorn, R. Wang, H. Chiu, A. L. Smirl, and H. Zhao, *Phys. Rev. B* **87**, 121406(R) (2013).
- [9] S. Hong, J. I. Dadap, N. Petrone, P. Yeh, J. Hone, and R. M. Osgood, Jr., *Phys. Rev. X* **3**, 021014 (2013).
- [10] J. J. Dean and H. V. van Driel, *Phys. Rev. B* **82**, 125411 (2010).
- [11] M. L. Nesterov, J. Bravo-Abad, A. Yu. Nikitin, F. J. Garcia-Vidal, and L. Martin-Moreno, *Laser Photonics Rev.* **7**, L7 (2013).
- [12] H. Dong, C. Conti, A. Marini, and F. Biancalana, *J. Phys. B: At. Mol. Opt. Phys.* **6**, 155401 (2013).
- [13] A. V. Gorbach, *Phys. Rev. A* **87**, 013830 (2013).
- [14] D. A. Smirnova, A. V. Gorbach, I. V. Iorsh, I. V. Shadrivov, and Yu. S. Kivshar, *Phys. Rev. B* **88**, 045443 (2013).
- [15] T. Gu, N. Petrone, J. F. McMillan, A. van der Zande, M. Yu, G. Q. Lo, D. L. Kwong, J. Hone, and C. W. Wong, *Nature Photon.* **6**, 554 (2012).
- [16] T. A. Birks, W. J. Wadsworth, and P. St. J. Russell, *Opt. Lett.* **25**, 1415 (2000).
- [17] X. Zhao, A. V. Gorbach, and D. V. Skryabin, *J. Opt. Soc. Am. B* **30**, 812 (2013).
- [18] A. Marini, R. Hartley, A. V. Gorbach, and D. V. Skryabin, *Phys. Rev. A* **84**, 063839 (2011).
- [19] G. P. Agrawal, *Nonlinear Fiber Optics*, 3rd ed. (Academic, 2001).
- [20] M. I. Katsnelson, *Graphene: Carbon in Two Dimensions* (Cambridge University Press, 2012).
- [21] M. Currie, J. D. Caldwell, F. J. Bezarez, J. Robinson, T. Anderson, H. Chun, and M. Tadjerb, *Appl. Phys. Lett.* **99**, 211909 (2011).
- [22] A. Reina, X. Jia, J. Z. Ho, D. Nezich, H. Son, V. Bulovic, M. Dresselhaus, and J. Kong, *Nano Lett.* **9**, 30 (2009).
- [23] D. Michaelis, U. Peschel, C. Wachter, and A. Brauer, *Phys. Rev. E* **68**, 065601 (2003).
- [24] R. M. Osgood Jr., N. C. Panoiu, J. I. Dadap, X. Liu, X. Chen, I.-W. Hsieh, E. Dulkeith, W. M. Green, and Y. A. Vlasov, *Adv. Opt. Photon.* **1**, 162 (2009).
- [25] S. V. Afshar and T. M. Monro, *Opt. Express* **17**, 2298 (2009).